NeuroImage: Clinical 23 (2019) 101946

Contents lists available at ScienceDirect

NeuroImage: Clinical

journal homepage: www.elsevier.com/locate/ynicl

# A study of neural activity and functional connectivity within the olfactory brain network in Parkinson's disease

Charalampos Georgiopoulos[a,b,*], Suzanne T. Witt[b], Sven Haller[c,d], Nil Dizdar[e], Helene Zachrisson[f], Maria Engström[b,g], Elna-Marie Larsson[d]

[a] Department of Radiology and Department of Medical and Health Sciences, Linköping University, Linköping, Sweden
[b] Center for Medical Image Science and Visualization (CMIV), Linköping University, Linköping, Sweden
[c] Centre Imagerie Rive Droite SA, Geneva, Switzerland
[d] Department of Surgical Sciences/Radiology, Uppsala University, Uppsala, Sweden
[e] Department of Neurology and Department of Clinical and Experimental Medicine, Linköping University, Linköping, Sweden
[f] Department of Clinical Physiology and Department of Medical and Health Sciences, Linköping University, Linköping, Sweden
[g] Department of Medical and Health Sciences, Linköping University, Linköping, Sweden

ARTICLE INFO

*Keywords:*
fMRI
Parkinson
Olfaction
Functional connectivity

ABSTRACT

Olfactory dysfunction is an early manifestation of Parkinson's disease (PD). The present study aimed to illustrate potential differences between PD patients and healthy controls in terms of neural activity and functional connectivity within the olfactory brain network. Twenty PD patients and twenty healthy controls were examined with olfactory fMRI and resting-state fMRI. Data analysis of olfactory fMRI included data-driven tensorial independent component (ICA) and task-driven general linear model (GLM) analyses. Data analysis of resting-state fMRI included probabilistic ICA based on temporal concatenation and functional connectivity analysis within the olfactory network. ICA of olfactory fMRI identified an olfactory network consisting of the posterior piriform cortex, insula, right orbitofrontal cortex and thalamus. Recruitment of this network was less significant for PD patients. GLM analysis revealed significantly lower activity in the insula bilaterally and the right orbitofrontal cortex in PD compared to healthy controls but no significant differences in the olfactory cortex itself. Analysis of resting-state fMRI did not reveal any differences in the functional connectivity within the olfactory, default mode, salience or central executive networks between the two groups. In conclusion, olfactory dysfunction in PD is associated with less significant recruitment of the olfactory brain network. ICA could demonstrate differences in both the olfactory cortex and its main projections, compared to GLM that revealed differences only on the latter. Resting-state fMRI did not reveal any significant differences in functional connectivity within the olfactory, default mode, salience and central executive networks in this cohort.

## 1. Introduction

Olfactory dysfunction has been associated with depression and several neurodegenerative disorders, such as Parkinson's disease (PD) and Alzheimer's disease (Barresi et al., 2012; Kohli et al., 2016; Smeets et al., 2009). Olfactory neural processing beyond the olfactory bulb is firstly conducted in the olfactory cortex, which includes the anterior olfactory nucleus, the olfactory tubercle, the piriform cortex, the amygdala and the entorhinal cortex; all of these brain regions receive direct, monosynaptic input from the olfactory bulb (Gottfried, 2010; van Hartevelt and Kringelbach, 2012). The piriform cortex is the largest structure within the olfactory cortex and can be divided, both anatomically and functionally, into the anterior piriform cortex and the posterior piriform cortex. Anterior piriform cortex is suggested to encode odorant identity, while posterior piriform cortex may encode odorant quality (Kadohisa and Wilson, 2006). Olfactory projections

*Abbreviations:* BOLD, Blood Oxygen Level Dependent; CI, Confidence Intervals; DaTSCAN, SPECT with the presynaptic ligand ioflupane; EPI, Echo planar imaging; FDR, False discovery rate; FIR, Finite Impulse Response; FLAIR, Fluid Attenuated Inversion Recovery; fMRI, functional Magnetic Resonance Imaging; FWHM, Full Width Half Maximum; GLM, General Linear Model; H&Y, Hoehn and Yahr Staging; MMSE, Mini-Mental State Examination; MNI, Montreal Neurological Institute; PD, Parkinson's disease; SPECT, Single Photon Emission Computed Tomography; TE, echo time; ICA, Independent Component Analysis; TR, repetition time; UPDRS, Unified Parkinson's Disease Rating Scale; UPSIT, University of Pennsylvania Smell Identification Test

* Corresponding author at: Röntgenkliniken, Universitetssjukhuset, Linköping 581 85, Sweden.
*E-mail address:* Charalampos.Georgiopoulos@regionostergotland.se (C. Georgiopoulos).

https://doi.org/10.1016/j.nicl.2019.101946
Received 13 December 2018; Received in revised form 23 June 2019; Accepted 17 July 2019
Available online 18 July 2019

beyond the olfactory cortex include the orbitofrontal cortex and anterior insula. The function of the orbitofrontal cortex is associated with odor discrimination, identification and memory; interestingly only the right orbitofrontal cortex is involved in conscious olfaction (Gottfried, 2010). Anterior insula is considered as a cognitive-evaluative area, which is often highly activated in studies requiring a task to be performed while smelling the olfactory stimulus (Seubert et al., 2013).

Olfactory loss in PD is not associated with changes in the nasal mucosa or the size of the olfactory bulb (Hummel et al., 2010b; Paschen et al., 2015). According to post-mortem studies in PD patients, Lewy bodies are present in the olfactory bulb, the anterior olfactory nucleus, the entorhinal cortex and the piriform cortex (Harding et al., 2002; Silveira-Moriyama et al., 2009). Olfactory dysfunction in PD is very common, occurs in early stages, often preceding the appearance of motor symptoms, and is independent of medication and age at onset (Doty et al., 1988; Hawkes et al., 1997, 1999; Tissingh et al., 2001). Hence, olfactory neuroimaging could potentially lead to the identification of PD-specific olfactory neural phenotypes, which could function as a prodromal biomarker of the disorder.

Functional Magnetic Resonance Imaging (fMRI) is a non-invasive imaging technique measuring the Blood Oxygen Level Dependent (BOLD) response to task-induced or spontaneous neural activity; the latter is commonly known as resting-state fMRI and it is often employed in studies of functional connectivity between different brain regions or networks. Since its inception, fMRI has been extensively used in a wide spectrum of cognitive and sensory studies, including olfaction. Even though it has been suggested that fMRI of human olfaction is not suitable as a diagnostic tool in single subjects, several studies have employed fMRI in order to identify the neural basis of olfactory dysfunction in both health and disease (Morrot et al., 2013; Pellegrino et al., 2016; Vasavada et al., 2017; Wang et al., 2005).

The association between PD and olfactory dysfunction has been studied with task-induced functional imaging and certain studies have tried to shed light on the underlying, disease-related, functional alterations in the olfactory cortex and its main projections in PD (Hummel et al., 2010a; Moessnang et al., 2011; Su et al., 2015; Welge-Lussen et al., 2009; Westermann et al., 2008). Results from previous olfactory fMRI studies are, however, inconsistent: two studies show declined activity in the olfactory cortex in PD, whereas one study reports hyperactivation of the olfactory cortex in early stages of PD (Hummel et al., 2010a; Moessnang et al., 2011; Westermann et al., 2008). This inconsistency can to a certain extent be attributed to methodological diversity, both in the experimental designs and in the analytical approaches.

Recently, there has been an increased interest in the applications of resting-state fMRI on PD, spanning from functional connectivity studies to studies of regional homogeneity. Independent component analysis (ICA) of resting-state fMRI has led to the identification of several, specific, large-scale brain networks that are recruited in most individuals, during a wakeful and resting state. The default mode, the salience and the executive network are only three of these large-scale networks, and they have been extensively investigated in several neurodegenerative and psychiatric diseases, including PD (Buckner et al., 2008; Chang et al., 2017; Lucas-Jimenez et al., 2016; Menon, 2011; Seeley et al., 2007). Anatomically, the default mode network includes the medial prefrontal cortex and the posterior cingulate cortex, the salience network consists of the insula and the anterior cingulate cortex, whereas the central executive network comprises the dorsolateral prefrontal cortex and the posterior parietal cortex. Functionally, the default mode network is associated with self-referential mental activity and it is typically deactivated during task-induced fMRI. The salience network is involved in the detection and filtering of external stimuli and internal brain events. The central executive network is often coactivated together with the salience network both at rest and during task performance; it plays a crucial role in working memory, problem solving and decision making. Resting-state fMRI has demonstrated altered functional coupling among these three networks in PD (Putcha et al., 2015).

Despite the advances in both olfactory and resting-state fMRI, it is still not fully understood how olfactory dysfunction in PD is reflected in the activation pattern of the olfactory network. Likewise, it is not fully investigated if olfactory dysfunction in PD is associated with potential changes in the functional connectivity within the olfactory, default mode and salience networks. Establishing a robust and reliable fMRI design is of high importance for the investigation of neural activity within the olfactory network. Our research group has previously studied the effects of stimulation length and MRI acquisition repetition time (TR) in the activation pattern of the olfactory cortex in healthy subjects, concluding that short stimulation length and short TR should be preferred in order to achieve maximum signal increase and short time to peak signal change (Georgiopoulos et al., 2018). In the present study, our previous methodological findings are applied in PD in order to elucidate potentially altered activation patterns and functional connectivity within olfactory brain areas. Our main hypothesis is that patients with PD show decreased activation in the piriform cortex, the orbitofrontal cortex and the anterior insula, decreased connectivity among these areas and decreased resting state activity in the salience, default mode and central executive networks, compared to healthy controls.

## 2. Methodology

### 2.1. Participants

Twenty PD patients (10 males) were recruited from the register of the Department of Nuclear Medicine at the University Hospital of Linköping, Sweden, where they had previously undergone single photon emission computed tomography (SPECT) with the presynaptic radiotracer ioflupane, also known as DaTSCAN® (GE Healthcare, Eindhoven, the Netherlands). DaTSCAN SPECT has been widely used as a diagnostic test to detect loss of functional dopaminergic neuron terminals in striatum. All PD patients that were recruited in this study demonstrated abnormal uptake of ioflupane. Twenty age-matched healthy controls (8 males) were recruited among patients' spouses or friends or through advertisements at the University Hospital of Linköping and at local non-political service organizations. All participants underwent olfactory evaluation prior to fMRI examination. All PD patients underwent the following clinical evaluation prior to fMRI: Mini-Mental State Examination (MMSE), motor examination according to the Movement Disorders Society–Sponsored revision of the Unified Parkinson's Disease Rating Scale (UPDRS, part III) and Hoehn and Yahr Staging (H&Y). On-off fluctuations of medical treatment were not explicitly monitored. However, all patients were encouraged to book their fMRI-examination during the part of the day that they usually had the best effect of their ongoing treatment. Inclusion criteria for PD patients were age between 55 and 75 years and MMSE score $> 25$. Inclusion criteria for healthy controls were age between 55 and 75 years and normal olfaction. Subjects with active colds or allergies, history of previous surgery in the nasal cavity, neurological disorders, mandibular implants or magnetic/electromagnetic implants (such as pacemakers) were excluded. Smokers were also excluded. Written informed consent was obtained from all participants. The study was conducted in accordance with the 1964 Helsinki declaration and its later amendments and was approved by the Regional Ethical Review Board (registration number 2018/144-32).

### 2.2. Olfactory evaluation

All participants underwent olfactory examination with the University of Pennsylvania Smell Identification Test (UPSIT, Sensonics, Inc., New Jersey, USA). This test consists of 40 different odorants, microencapsulated in booklets. On each page there is one odorant,

embedded in a microcapsule, and a multiple-choice question with four alternative responses. The odorant is released by scratching the microcapsule, and the tested subject is then required to choose the best fitted alternative. The performance of each patient is presented as UPSIT score, which has a range from 0 to 40.

### 2.3. DaTSCAN

Image acquisition, processing and automated semi-quantitative evaluation were performed as previously described by our group (Davidsson et al., 2014). Before isotope administration, all patients received 120 mg of sodium perchlorate per os to block uptake of iodine in the thyroid. One hour later 185 MBq DaTSCAN was given intravenously; SPECT was performed 3–4 h after DaTSCAN administration with a dual-head, multi-geometry gamma camera (Millennium VG, GE Healthcare). The two camera heads were positioned as close as possible to patient's head. All collected transaxial SPECT images were assessed visually and were classified in accordance with Kahraman's proposed scale, which includes 5 distinct patterns (Kahraman et al., 2012): a) burst striatum: severe bilateral reduction, with almost no uptake in putamen or caudate nucleus and increased, non-specific background uptake, b) egg shape: bilateral uptake reduction in both putamina and normal or borderline normal uptake from caudate nucleus, c) mixed type: asymmetrical ioflupane uptake, with reduced uptake in the putamen of one side, d) eagle wing: borderline normal, symmetrical ioflupane uptake, with only discrete reduction in one or both putamina, and e) normal: symmetrical ioflupane uptake in putamen and caudate nucleus bilaterally.

### 2.4. fMRI data acquisition

FMRI was performed with a 3 T scanner (Siemens MAGNETOM Prisma, Siemens AG, Erlangen, Germany) using a 20-channel head-neck coil. A multiplex echo planar imaging (EPI) sequence, including an initial fat saturation pulse, was used for both the olfactory fMRI and the resting-state fMRI: TR/echo time (TE) = 901/30 ms; flip angle = 59°; simultaneous multi slice = 2; integrated parallel acquisition technique = 2; EPI factor = 128; field of view = 192 × 192 $mm^2$; matrix = 64 × 64; # slices = 48; slice thickness (gap) = 3 (0) mm; voxel = 3x3x3 $mm^3$. For the olfactory fMRI, 590 time points were collected (total scan time = 531.59 s). For the resting-state fMRI, 660 time points were collected (total scan time = 594.66 s). Additionally, high-resolution 3D T1-weighted and T2-weighted Fluid Attenuated Inversion Recovery (FLAIR) structural scans were acquired in all subjects. T1-weighted images were later coregistered with the functional images. T2-weighted FLAIR images were acquired to ensure that the participants did not have any obvious, co-morbid, pathological changes in the brain that might have resulted in olfactory dysfunction (i.e. intracranial tumors, ischemic and traumatic lesions). White matter lesions were assessed with the Fazekas rating scale (healthy controls: median grade 1, 95% CI:1 and 1; PD patients: median grade 1, 95% CI:1 and 1) (Wahlund et al., 2001). Brain atrophy was assessed with the Global Atrophy Scale (healthy controls: median grade 1, 95% CI: 1 and 1; PD patients: median grade 1, 95% CI: 1 and 2) (Pasquier et al., 1996). There were no significant differences between the groups in terms of white matter lesions or brain atrophy.

### 2.5. Olfactory fMRI design

Two odorants were employed during the task-induced fMRI: natural coffee oil extract and vanillin (Sigma-Aldrich, St. Louis, USA). Both coffee oil extract (40% v/v) and vanillin (10% w/v) were diluted in odorless diethyl phthalate (Sigma-Aldrich). Stimulation was administered in blocks of events, with 6 s stimulus length. Both odorants were randomly embedded in the same session (Fig. 1), which included 10 blocks for each odorant. A 20 s long resting period, consisting of odorless air, separated the stimulation blocks from each other. To avoid habituation, each stimulation block consisted of 1 s long odorous pulses, followed by 2 s of odorless air. The odorant was delivered simultaneously to both nostrils, using the OG001 Multistimulator (Burghart Messtechnik GmbH, Wedel, Germany), embedded in medical air stream (2.5 l airflow per nostril), through Teflon-tubing (4 mm inner diameter). To remove residual odorants, a constant, inverse airflow was maintained inside the magnet aperture. All subjects were instructed to breathe normally through the nose and avoid sniffing. All participants were asked to click a button with their index finger every time they could sense the smell of coffee or vanillin in order to objectively confirm odor sensation. Registration of response was open for 13 s, 1 s prior to stimulation, during stimulation and 6 s after, in order to ensure that even very early or very delayed responses (due to motor deficit in PD) would be registered.

### 2.6. Analysis of olfactory fMRI

Three analytical approaches were employed for the analysis of olfactory fMRI: a) model-free ICA, b) task-driven general linear model (GLM) analysis, and c) extracting the event related time course of brain activation in four olfactory brain areas.

ICA was carried out with MELODIC version 3.15, part of FSL 6.0 (FMRIB Analysis Group, University of Oxford, UK). Tensorial ICA allows a model-free decomposition of the variance in the signal, into different activation and artefactual components, including their spatial maps and time courses (Beckmann and Smith, 2005). The following data pre-processing was applied to the input data: correction for head motion with the intramodal Motion Correction using FMRIB's Linear Image Registration Tool (MCFLIRT); masking of non-brain voxels; voxel-wise de-meaning of the data; normalization of the voxel-wise variance; pre-processed data were whitened and projected into a 20-dimensional subspace using Principal Component Analysis, in both first and second level analysis. The whitened observations were decomposed into sets of vectors that describe signal variation across the temporal domain (time courses), the session/subject domain and across the spatial domain (maps) by optimizing for non-Gaussian spatial source distributions using a fixed-point iteration technique (Hyvarinen, 1999). Estimated Component maps were divided by the standard deviation of the residual noise and thresholded by fitting a mixture model to the histogram of intensity values (Beckmann and Smith, 2004). We chose to separate the signal into 20 independent components, based on previous research indicating that a dimensionality of 20 components provides a general picture of large-scale brain networks (Abou-Elseoud et al., 2010; Ray et al., 2013; Smith et al., 2009). Each independent component consists of a thresholded spatial map, a time-course (temporal mode) and an s-mode (measure of the effect size of each independent component for each participant). Comparison of the s-modes of the two groups was performed to test for differences in the effect size between PD patients and healthy controls.

GLM analysis was carried out with SPM12 (Wellcome Trust Centre for Neuroimaging, University College London, London, UK). All participants' images were separately realigned and the translation and rotation correction parameters were individually examined to ensure that no participant had significant head motion larger than one voxel in any direction. No participants were excluded due to head motion. Spatial normalization into Montreal Neurological Institute (MNI) space was initially performed on the anatomical T1-weighted image of each participant, and these normalization parameters were then applied to each respective functional image set. The normalized images were smoothed with an 8 mm full width half maximum (FWHM) Gaussian kernel. The stimulation blocks were modeled as regressors of interest, one for each odorant (coffee and vanillin). The resting periods were not explicitly modeled. The six motion parameters derived from the realignment step were included as covariates of no interest. At second level analysis, healthy controls and PD patients were compared separately for each

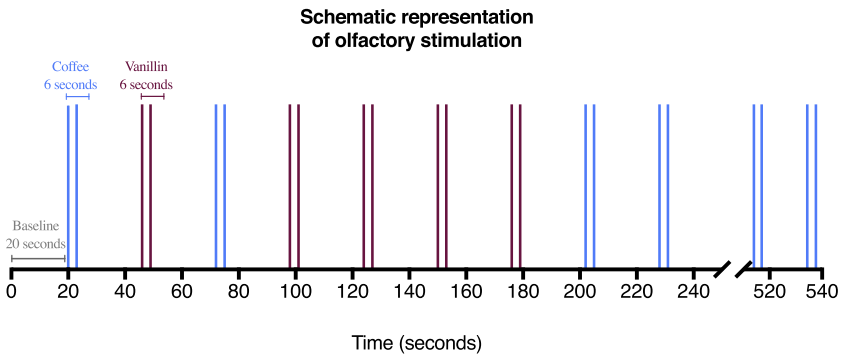


**Fig. 1.** Schematic representation of the olfactory fMRI design. Two odorants, coffee and vanillin (10 blocks of events for each length), were randomly embedded in one session. A 20 s long resting period (baseline), consisting of odorless air, separated the stimulation blocks from each other. To avoid habituation, each stimulation block consisted of 1 s long odorous pulse, followed by 2 s of odorless air.

contrast (coffee, vanillin) with a 2-samples *t*-test, but also with ANOVA for the combination of both contrasts. Additionally, we performed a GLM analysis by focusing only on the detected stimuli, e.g. the stimuli with positive response based on the response tracking, which were modeled as regressors of interest on the first level. At second level analysis, we performed a two-sample t-test between healthy participants and PD patients.

Subsequently, the Finite Impulse Response (FIR) event time courses were plotted for four different olfactory brain areas: the anterior piriform cortex, the posterior piriform cortex, the orbitofrontal cortex and the anterior insula. ROI analysis was carried out with MarsBaR 0.44 toolbox for SPM, on the GLM-analyzed data. The ROIs were designed in accordance with a previously described statistical localization of the human olfactory cortex (Seubert et al., 2013). Firstly, the point with the peak activity was identified for each participant in each ROI, separately for each odorant, in both the right and the left hemisphere. The coordinates from all these points were used as the center of a small spherical cluster with 2 mm radius, so that a unique sphere was designed for each participant, each odorant and each ROI. At last, the following three components of all the time courses were calculated separately for each ROI: maximal signal change, time-to-peak and area under the curve (only the area and the first 10 s of the curve were included).

### 2.7. Analysis of resting-state fMRI

Before analyzing the resting-state fMRI data, framewise displacement was calculated for all participants (Power et al., 2012). Two healthy controls and two PD patients were excluded from further analysis because of framewise displacement > 2 mm in several timepoints. The remaining data (18 healthy controls, mean framewise displacement 0.14 mm ± 0.10; 18 PD patients, mean framewise displacement 0.15 mm ± 0.10; no significant difference between groups) were further assessed with two analytical approaches: a) functional connectivity analysis among the four abovementioned olfactory brain ROIs, and b) ICA in order to identify the default mode, the salience and the central executive network.

For functional connectivity analysis, we used the default pipeline of the CONN toolbox (http://www.nitrc.org/projects/conn), that implements the component-based noise correction method (aCompCor) strategy for reduction of physiological and other source noise, additional removal of movement and temporal covariates, temporal filtering and windowing of the residual BOLD signal, first-level estimation of multiple standard functional connectivity measures, and second-level random-effect analysis for resting state data (Whitfield-Gabrieli and Nieto-Castanon, 2012). The ART-based scrubbing method, implemented in CONN, was further used to detect outlying volumes with high motion, using a 2 mm subject motion threshold (average scrubbing: healthy controls 21 volumes ± 17, PD patients 13 volumes ± 10). Segmented white matter and cerebrospinal fluid were entered as confounds along with realignment parameters in a first-level analysis, and the data were band-pass filtered to 0.008 Hz – 0.09 Hz. We then conducted a ROI-to-ROI analysis to test the hypothesis regarding the functional connectivity among the same four olfactory ROIs mentioned above; as with the FIR event time courses, we used previously described statistical localization of the human olfactory cortex (Seubert et al., 2013). CONN computed temporal correlations between the BOLD signals in these four ROIs. This procedure was applied to both PD patients and healthy controls. Two-way between groups (PD vs. healthy controls) *t*-tests were run to examine whether differences in connectivity strength between groups were present, with the UPSIT score serving as covariate. False discovery rate (FDR; $p < .05$) was used to correct for multiple comparisons.

Probabilistic ICA, as implemented in MELODIC version 3.15, part of FSL 6.0, was carried out in an effort to separate the signal into resting-state networks and, then, identify the default, the salience and the central executive network in this cohort. As opposed to tensorial ICA, which was used in the olfactory fMRI since the stimulus paradigm was consistent among subjects, for the resting-state fMRI we used the temporal concatenation to look for common spatial patterns, without assuming that the temporal response is consistent among subjects. The following default data pre-processing pipeline was applied to the input data: masking of non-brain voxels, voxel-wise de-meaning of the data, and normalization of the voxel-wise variance. Pre-processed data were whitened and projected into a 20-dimensional subspace using Principal Component Analysis, in both first and second level analysis. The whitened observations were decomposed into sets of vectors which describe signal variation across the temporal domain (time-courses), the session/subject domain and across the spatial domain (maps) by optimizing for non-Gaussian spatial source distributions using a fixed-point iteration technique (Hyvarinen, 1999). Estimated Component maps were divided by the standard deviation of the residual noise and thresholded by fitting a mixture model to the histogram of intensity values (Beckmann and Smith, 2004). Thereafter, the set of spatial maps from the group-average analysis was used to generate subject-specific versions of the spatial maps, and associated timeseries, using dual regression (Nickerson et al., 2017). First, for each subject, the group-average set of spatial maps was regressed (as spatial regressors in a multiple regression) into the subject's 4D space-time dataset. This resulted in a set of subject-specific timeseries, one per group-level spatial map. Next, those timeseries were regressed (as temporal regressors, again in a multiple regression) into the same 4D dataset, resulting in a set of subject-specific spatial maps, one per group-level spatial map. We then employed FSL's randomize permutation-testing tool to test for differences between PD patients and healthy controls, with the UPSIT score serving as covariate. Additionally, we tested for potential correlation between the UPSIT score and the recruitment of the default mode, the salience and the central executive networks.

### 2.8. Statistics

Potential differences between groups regarding age, olfactory

testing, response monitoring, the FIR event related time courses and the s-modes of ICA were investigated with Mann-Whitney *U* test, since these data were not normally distributed (Shapiro-Wilk test). Fisher's exact test was employed to investigate potential differences in sex and MMSE score. Potential correlation between the UPSIT score and the s-modes of ICA for all participants, as well as between the UPDRS score and the s-modes of ICA for PD patients were calculated with the Spearman correlation coefficient. Statistical analysis of the behavioral data and the FIR event related time courses was performed with IBM SPSS Statistics version 25. All plots were created in GraphPad® Prism 7. All results presented in the text represent the median value with lower and upper 95% confidence intervals (CI). The FIR event related time courses represent percentage of signal change by time. Statistical significance for the analysis of FIR event related time courses was set at $p < .05$. For the GLM analysis, whole brain analysis was assessed at $p < .001$. The default threshold level of $p > .5$ was used for ICA in order to test the alternative hypothesis post-statistically.

## 3. Results

### 3.1. Demography and behavioral data

The demographics of both PD patients and healthy controls are summarized in Table 1. There was no significant difference regarding gender or age between the two groups. The median value of the UPSIT score was 18.5 out of 40 (95% CI 14 and 23) for the PD group and 33 out of 40 (95% CI 32 and 35) for the healthy controls. Mann-Whitney *U* test showed that PD patients had significantly lower UPSIT score than healthy controls ($p < .001$).

All participants were asked to verify the presence of odor during the olfactory fMRI, by pressing a button with their index finger. The number of total responses and the mean reaction time were collected separately for coffee and vanillin. The results of response monitoring are summarized in Table 2. Statistical analysis with the Mann-Whitney U test showed that PD patients gave significantly fewer responses for the combination of both odors ($p = .028$) and for coffee ($p = .041$). There were no significant differences in the number of responses for vanillin or in the mean reaction time for each odor.

### 3.2. DaTSCAN

All PD patients underwent DaTSCAN SPECT examination prior to inclusion in the study and they all demonstrated abnormal ioflupane uptake. DaTSCAN images were classified into five distinct uptake patterns, as mentioned in Section 2.3. Thirteen PD patients were visually classified as “egg shape”, i.e. bilateral uptake reduction in both putamina and normal or borderline normal uptake from caudate nucleus, whereas seven PD patients were visually classified as “mixed type”, i.e. asymmetrical ioflupane uptake, with reduced uptake in the putamen of one side.

**Table 1**
Demographics (median and 95% confidence intervals). UPSIT: University of Pennsylvania Smell Identification Test, MMSE: Mini-Mental State Examination, UPDRS: Unified Parkinson's Disease Rating Scale.

| | PD | Healthy |
|---|---|---|
| Participants | 20 | 20 |
| Age (years) | 67 (63–70) | 66.5 (62–69) |
| Sex (male/female) | 10/10 | 8/12 |
| UPSIT score (out of 40) | 18.5 (14–23) | 33 (32–35) |
| MMSE | 28.5 (28–29) | – |
| UPDRS part III | 20 (16–21) | – |
| Hoehn & Yahr | 2 (2–2.5) | – |

**Table 2**
Response tracking (median and 95% confidence intervals).

| | PD | Healthy |
|---|---|---|
| Total responses for both odors (out of 20) | 12 (7–17) | 16 (13–19) |
| Responses for coffee (out of 10) | 8 (5–10) | 10 (9–10) |
| Mean reaction time for coffee (seconds) | 3.2 (2.6–3.8) | 3.1 (2.6–3.7) |
| Responses for vanillin (out of 10) | 3.5 (2–8) | 8 (5–9) |
| Mean reaction time for vanillin (seconds) | 2.1 (1–4) | 2.9 (2.1–3.6) |

### 3.3. Olfactory fMRI

Table 3 summarizes the 20 independent components that tensorial ICA isolated. One of these components was associated with a functionally connected olfactory network, including the posterior piriform cortex, the insula and the thalamus bilaterally, as well as the right orbitofrontal cortex (Fig. 2a). The hand motor area of the left precentral gyrus was also part of this network, due to the response monitoring task. This component was responsible for 7.8% of the explained variance of the signal. The time course of this component consisted of an oscillation with 21 distinct peaks, coinciding with the olfactory stimulation of the tested fMRI task design (Fig. 2b); the first peak occurred prior to olfactory stimulation and was probably associated with the sensation of odorless air at the beginning of the fMRI design (Fig. 1). The s-mode values of all participants were compared to test differences in the effect size of this component between healthy controls and PD patients; healthy controls had significantly higher s-mode values compared to PD patients ($p = .014$, Fig. 2c).

Additionally, ICA isolated a cerebellar functional network, consisting of the posterior and lateral parts of cerebellum bilaterally (Fig. 3a). This component was responsible for 6.52% of the explained variance of the signal. The time course of this component consisted of an oscillation with 21 distinct peaks, coinciding with the olfactory stimulation of the tested fMRI task design (Fig. 3b). Comparison of the s-mode values showed that healthy controls recruited this cerebellar network significantly more compared to PD patients ($p = .026$, Fig. 3c). None of the s-modes of these two networks (olfactory and cerebellar) was significantly correlated with the UPSIT or the UPDRS score.

Collected data were also analyzed with GLM, using two different contrasts: coffee and vanillin. For vanillin, healthy controls showed higher activation in parts of right insula ($p < .001$, uncorrected; Fig. 4a). For coffee, healthy controls showed higher activation in parts of right insula and right orbitofrontal cortex ($p < .001$, uncorrected; Fig. 4b). For the combination of both coffee and vanillin, healthy controls showed higher activation in parts of insula bilaterally and for parts of the right orbitofrontal cortex ($p < .001$, uncorrected; Fig. 4c). There were no significant differences between healthy controls and PD patients in any of the piriform cortices for any of the contrasts. In all cases (vanillin, coffee and the combination of them) healthy controls showed higher activation in the hand motor area of the left precentral gyrus, as well as the posterior limb of the left internal capsule, due to the response monitoring task (not illustrated in Fig. 4). Supplementary GLM analysis was performed by focusing only on the detected stimuli, as monitored by response tracking. In this case, there were no significant differences between the two groups in any olfactory brain region.

Lastly, the FIR event related time courses were extracted from the normalized fMRI data, for the following four olfactory brain areas: the anterior and the posterior piriform cortex, the orbitofrontal cortex and the insula. In order to compare the time courses between the two groups, three parameters were assessed statistically: maximal signal change, time-to-peak and area under the curve (only for the first 10 s). Healthy controls demonstrated higher maximal signal change compared to PD patients in the right orbitofrontal cortex ($p = .007$), the right insula ($p = .008$) and the left insula ($p = .045$). Healthy controls also demonstrated broader area under the curve compared to PD patients in

**Table 3**
Summary of the 20 independent components (IC) that were isolated by the tensorial Independent Component Analysis of the olfactory fMRI, including the explained variance of the signal, the effect size (s-mode) for each component (separately for healthy controls and PD patients), the *p*-value from the Mann-Whitney *U* test (only when $p < .05$) and the maximum spectral power (including the frequency in which that occurred). IC 6 was an olfactory component. IC 7 was a cerebellar component. n.s.: not significant, SD: standard deviation.

| IC | Explained Signal Variance | s-mode healthy controls | | s-mode PD patients | | p | Spectral Power | |
|---|---|---|---|---|---|---|---|---|
| | | mean | SD | mean | SD | | Max power | frequency (Hz/100) |
| 1 | 15.29% | 2.009 | 0.974 | 2.036 | 0.987 | n.s. | 5397 | 1.316 |
| 2 | 15.02% | 2.041 | 0.896 | 1.813 | 1.166 | n.s. | 13,292 | 3.76 |
| 3 | 14.66% | 1.762 | 0.786 | 1.910 | 0.888 | n.s. | 8637 | 3.948 |
| 4 | 14.41% | 1.947 | 0.878 | 1.990 | 1.012 | n.s. | 8375 | 3.76 |
| 5 | 11.84% | 1.662 | 0.737 | 1.662 | 0.728 | n.s. | 9162 | 3.948 |
| 6 | 7.80% | 1.708 | 1.088 | 0.715 | 1.321 | 0.014 | 81,240 | 3.76 |
| 7 | 6.52% | 1.461 | 0.943 | 0.503 | 1.635 | 0.026 | 60,551 | 3.76 |
| 8 | 5.54% | 0.886 | 0.899 | 1.051 | 0.835 | n.s. | 8432 | 0.94 |
| 9 | 4.43% | 0.900 | 1.869 | 0.594 | 0.596 | n.s. | 41,798 | 0.376 |
| 10 | 2.26% | 0.155 | 1.790 | 0.179 | 0.691 | n.s. | 11,236 | 2.444 |
| 11 | 1.37% | 0.546 | 1.945 | 0.097 | 0.463 | n.s. | 9422 | 2.632 |
| 12 | 1.26% | 0.775 | 1.941 | 0.204 | 0.569 | n.s. | 20,291 | 0.376 |
| 13 | 1.00% | 0.681 | 2.562 | 0.084 | 0.197 | n.s. | 5136 | 2.256 |
| 14 | 0.62% | 0.408 | 1.491 | 0.048 | 0.115 | n.s. | 3571 | 18.8 |
| 15 | 0.24% | 0.002 | 0.388 | 0.807 | 3.270 | n.s. | 6113 | 11.656 |
| 16 | 0.11% | −0.255 | 1.210 | 0.425 | 1.099 | n.s. | 8335 | 22.184 |
| 17 | 0.29% | −0.066 | 0.256 | 0.419 | 1.491 | n.s. | 7385 | 19.928 |
| 18 | 0.50% | −0.066 | 0.373 | 0.637 | 3.160 | n.s. | 3783 | 27.824 |
| 19 | 0.59% | 0.004 | 2.229 | 0.033 | 0.719 | n.s. | 32,786 | 0.94 |
| 20 | 0.99% | 0.217 | 1.760 | −0.170 | 0.660 | n.s. | 48,103 | 0.752 |

the right orbitofrontal cortex ($p = .044$), the right insula ($p = .045$) and the left insula ($p = .041$). There were no significant differences for the time-to-peak between subjects. Additionally, potential differences between the two odors were tested for the same three parameters, without yielding any significant differences between coffee and vanillin. The FIR event related time courses for the insula bilaterally and for the right orbitofrontal cortex are illustrated in Fig. 5.

### 3.4. Resting-state fMRI

Functional connectivity analysis among the same four olfactory brain areas (anterior and posterior piriform cortex, orbitofrontal cortex and insula) was performed with the CONN toolbox, using the UPSIT score as covariate. There were no significant differences between healthy controls and PD patients in terms of functional connectivity among these four brain areas. The temporal concatenation approach of ICA yielded three independent components, corresponding to the salience network (insula and anterior cingulate cortex), the default mode network (medial prefrontal cortex and posterior cingulate cortex) and the central executive network (dorsolateral prefrontal cortex and posterior parietal cortex) of this cohort. Dual regression analysis, with the UPSIT score as covariate, demonstrated no significant differences between healthy controls and PD patients for any of these networks. There was a tendency for positive correlation ($p = .08$) between the UPSIT score and the recruitment of the central executive network, however not statistically significant.

## 4. Discussion

We employed multi-analytical approaches on both olfactory and resting-state fMRI to test our main hypothesis that PD patients demonstrate decreased activation in olfactory brain areas and decreased connectivity within the olfactory, the salience and the default mode networks. ICA of olfactory fMRI isolated an olfactory and a cerebellar network, with significantly lower recruitment in PD patients compared to healthy controls. According to the task-driven GLM analysis, PD patients demonstrated decreased activation of the insula bilaterally and the right orbitofrontal cortex, but not in the olfactory cortex itself. The analysis of resting-state fMRI did not yield any significant differences in the connectivity within the olfactory, the salience and the default mode networks, between the two groups.

### 4.1. Olfactory fMRI

As most odorants differentially stimulate both the olfactory and the trigeminal nerve, choosing stimulants for olfactory fMRI needs to be thorough. Vanillin is generally considered as a purely olfactory stimulant (Brand, 2006). In fact, a study of 47 odorants demonstrated that only vanillin and decanoic acid could not be detected by anosmic patients, indicating that these two odorants possess no trigeminal component (Doty et al., 1978). Even though coffee has both olfactory and trigeminal components, it was a relevant choice in this cohort since abnormal olfaction has been associated with lower lifetime caffeine consumption in first-degree relatives of PD patients (Siderowf et al., 2007). Both vanillin and coffee were considered as familiar and pleasant odorants by the participants of this study. The analysis of the FIR event related time courses showed no significant differences between these two odors in the olfactory brain areas studied here, despite the fact that these odors have different evocative properties. Selective hyposmia in PD has been a controversial topic. Some studies support that specific odors appear specifically affected in PD, while others reject it as a reliable method to detect PD (Bohnen et al., 2008; Bohnen et al., 2007; Hahner et al., 2013). The findings of this study do not support the theory of selective hyposmia.

Response monitoring during the olfactory fMRI was employed as an objective measure of chemosensation during the experiment. PD patients gave significantly fewer responses compared to healthy participants during the whole session (for both coffee and vanillin), as well as for coffee alone. There was no significant difference for vanillin, which could possibly be explained by two factors: a) the purely olfactory nature of this odorant, b) the lower concentration of vanillin compared to that of coffee, making the detection of vanillin difficult even for healthy participants (all participants were instructed to push the button only when they could certainly smell an odor). The absence of significant differences in the mean reaction time between the two groups indicates that the significantly different number of responses cannot be attributed to PD patients' motor deficit. The GLM analysis support the findings from response monitoring since PD patients showed decreased

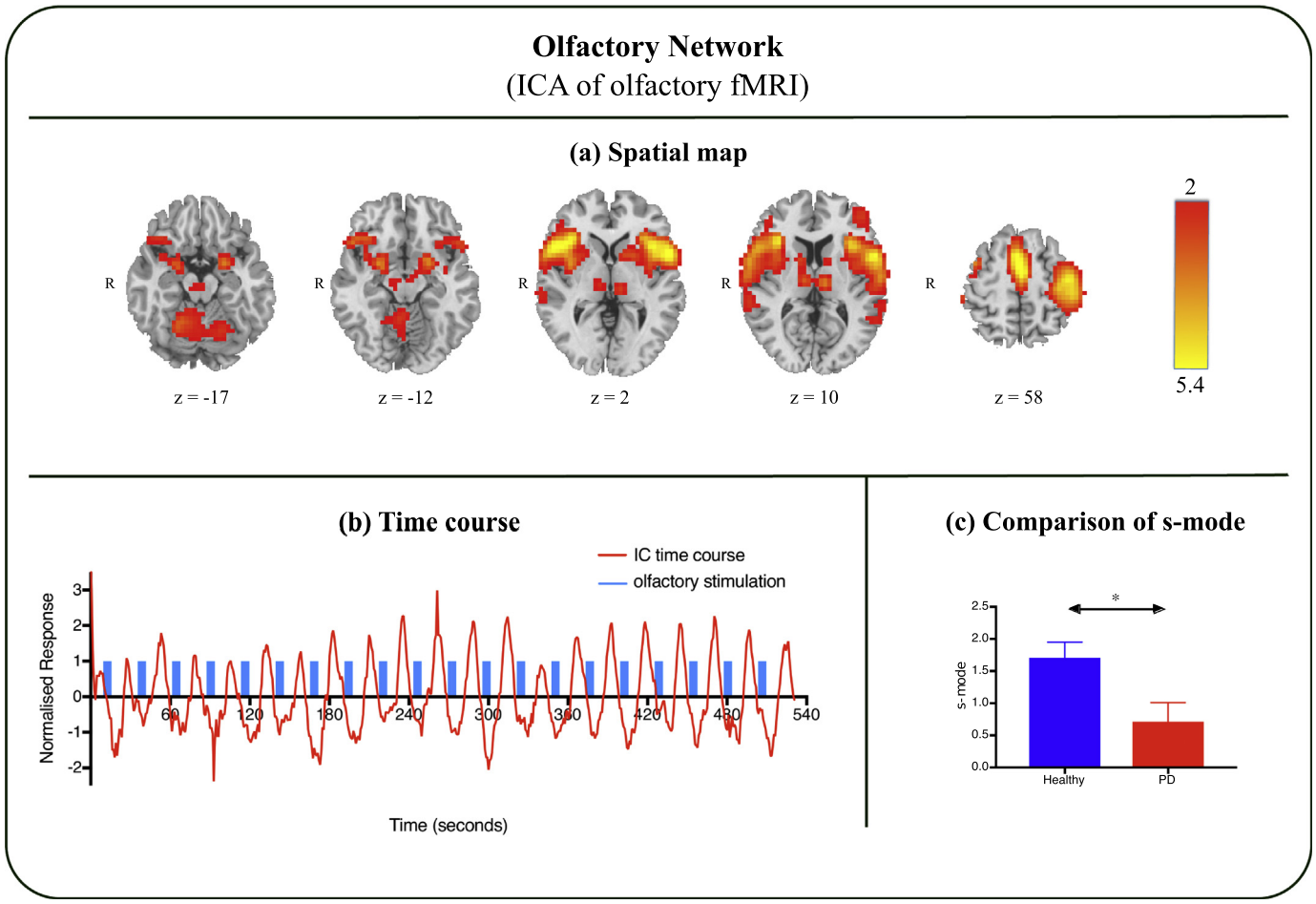


**Fig. 2.** The olfactory network as isolated with Independent Component Analysis (ICA) of the olfactory fMRI. (A) One independent component was associated with an olfactory network, consisting of the posterior piriform cortex, anterior insula and thalamus bilaterally, as well as the right orbitofrontal cortex. The hand motor area of the left precentral gyrus was also part of this network, due to the response monitoring task. (B) This independent component (IC) coincided temporally (time course in red) with the olfactory stimulation of the tested fMRI task design (blue). (C) The s-mode values (measure of the effect size for each participant) were significantly higher in healthy controls than PD patients (p = .014). Color bars are given in terms of T-statistic. R: right hemisphere. The spatial brain map was created with FSLeyes (FMRIB Analysis Group, University of Oxford, UK).

activation in the hand motor area of the left precentral gyrus and the posterior limb of the left internal capsule for all contrasts (vanillin, coffee, and their combination).

ICA is able to identify functionally connected brain regions, without predefining the hemodynamic response function or the design matrix. On the other hand, GLM employs the canonical hemodynamic response function for all brain regions and it is dependent of an a priori specified design matrix. ICA is, therefore, considered to be superior of GLM when there is uncertainty about the position and the timing of activity, due to condition-dependent, brain region-dependent, or subject-dependent variations (Bartels and Zeki, 2004). In this study, ICA was able to detect a functional network that consisted of both the olfactory cortex (posterior piriform cortex) and its main projections (insula and thalamus bilaterally, right orbitofrontal cortex), and it coincided temporally with the design of the olfactory fMRI. Additionally, PD patients demonstrated significantly lower recruitment of this network (lower s-mode values) compared to healthy controls. GLM and FIR event related time course analysis showed decreased activation in main olfactory projections (insula bilaterally and right orbitofrontal cortex), but no significant differences in the olfactory cortex itself. Moreover, the GLM results were only significant at the uncorrected $p < .001$ level; after correcting for false positives (family-wise error rate) there were no significant differences between the groups in any olfactory brain area. Hence, ICA was more effective for detecting olfactory impairment in this cohort, in both the olfactory cortex and its main projections. It should however be noted that ICA was performed with the default post-stats level of 0.5, meaning an equal loss on false positives and false negatives.

Supplementary GLM analysis, focusing only on the stimuli that were detected by the participants of this study, did not yield any significant differences between the two groups. This is essentially an expected finding, indicating that PD patients, despite their impaired olfaction, can still employ the same olfactory brain areas when the odorous stimulus is perceived. This finding provides further evidence that differences observed with ICA can be attributed to the undetected odorous stimuli, and, thus, reflect impaired olfaction in PD.

Cerebellar activation due to olfactory stimulation, as well as olfactory impairment in patients with cerebellar lesions have been previously described (Abele et al., 2003; Connelly et al., 2003; Sobel et al., 1998; Zatorre et al., 2000). Cerebellum is considered to be involved in the control of sniffing, and thereby it may also play a role in higher-order olfactory processing (Mainland and Sobel, 2006). Sobel et al. have demonstrated odor-induced activation posteriorly and laterally in the cerebellar hemispheres, independently of sniffing, supporting the argument that sniffing is more than a merely stimulus carrier (Sobel et al., 1998). Additionally, a recent study in hyposmic and anosmic patients shows correlation between the recruitment of the cerebellar network and the olfactory function scores of the patients (Reichert

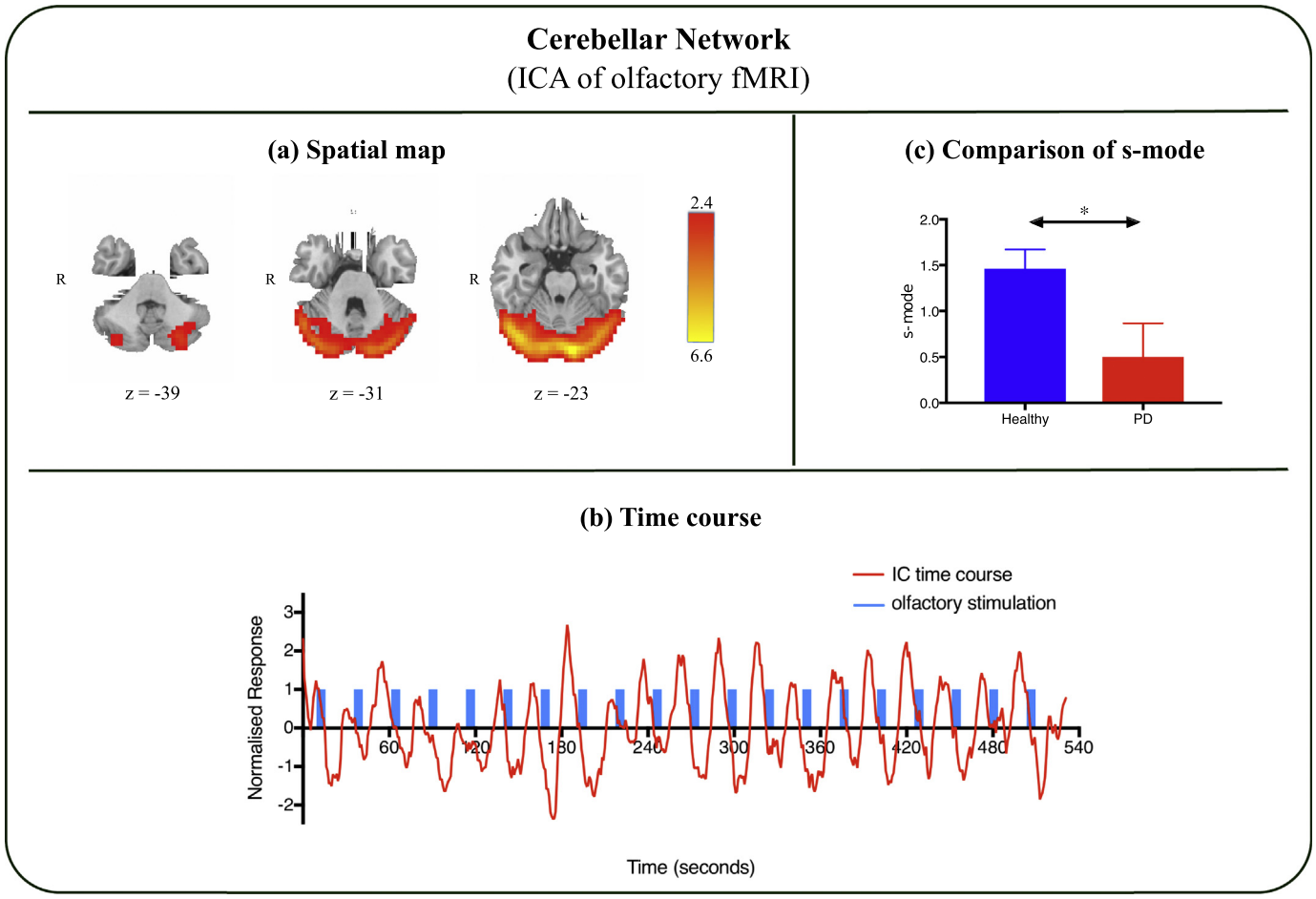


**Fig. 3.** The cerebellar network as isolated with Independent Component Analysis (ICA) of the olfactory fMRI. (A) One independent component was associated with a cerebellar network, consisting of the posterior and lateral parts of cerebellum bilaterally. (B) This independent component (IC) coincided temporally (time course in red) with the olfactory stimulation of the tested fMRI task design (blue). (C) The s-mode values (measure of the effect size for each participant) were significantly higher in healthy controls than PD patients ($p = .026$). Color bars are given in terms of T-statistic. R: right hemisphere. The spatial brain map was created with FSLeyes (FMRIB Analysis Group, University of Oxford, UK).

et al., 2018). Interestingly, PD patients demonstrate both sniffing and olfactory impairment (Sobel et al., 2001). This study verifies the recruitment of a cerebellar network during olfactory fMRI, and indicates that its recruitment is weaker in PD patients. However, it should be noted that the response monitoring task during the olfactory fMRI, could also be partially responsible for the recruitment of the cerebellar network.

There is currently a limited number of task-induced fMRI studies focusing on olfactory dysfunction in PD. Their task-designs differ considerably and their results are to some extent contradictive. Two studies have shown reduced activity in the amygdalo-hippocampal complex in PD patients, both with pleasant and unpleasant odors (Hummel et al., 2010a; Westermann et al., 2008). However, Moessnang et al. have shown a profound hyperactivation of the piriform and the orbitofrontal cortices in early stages of PD (Moessnang et al., 2011). Interestingly, these three studies employed solely GLM analysis. Both ICA and GLM analysis in this study indicate that olfactory impairment in PD is in line with decreased activation in the olfactory cortex and its main projections in the brain.

### 4.2. Resting-state fMRI

The default mode network has been suggested to have a key role in cognitive processing, whereas the salience network is considered to be responsible for detecting external and internal information in order to maintain goal-directed behavior (Raichle and Snyder, 2007; Seeley et al., 2007). The central executive network is associated with working memory and attention and its activity is often positively correlated with that of the salience network (Menon, 2011). On the other hand, the central executive network is normally anti-correlated with the default mode network.

This functional coupling is proven to be altered in PD, with PD patients presenting higher coupling between the default mode and the central executive network (Putcha et al., 2015). Additionally, impaired coupling between the salience and the default mode networks has been associated with cognition deficits in PD (Putcha et al., 2016). In another resting-state fMRI study, PD patients demonstrated decreased functional connectivity in the default mode network compared to healthy controls, but no significant differences in the central executive network (Disbrow et al., 2014). Reduced functional connectivity within the default mode network has also been associated with lower cognitive performance in PD patients, especially in the rigidity-predominant subtype (Hou et al., 2016; Karunanayaka et al., 2016; Lucas-Jimenez et al., 2016). Furthermore, decreased volume of the salience network, in particular the insular part, has been implicated in the presence of depression in PD patients with mild cognitive impairment (Chang et al., 2017).

There has been evidence that olfactory processing deactivates the default mode network in task-induced fMRI (Karunanayaka et al., 2017), but to our knowledge there is no previous resting-state fMRI

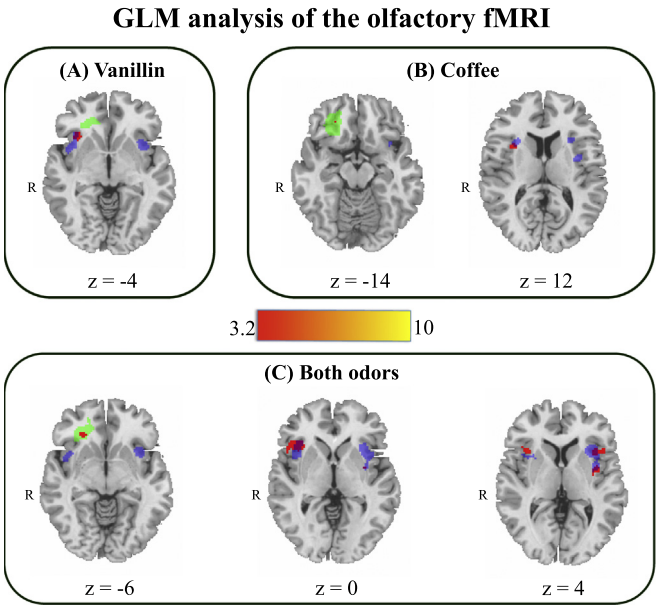


**Fig. 4.** Thresholded maps from the General Linear Model (GLM) analysis of the olfactory fMRI. (A) For vanillin, healthy controls showed higher activation in parts of right insula. (B) For coffee, healthy controls showed higher activation in parts of right insula and right orbitofrontal cortex. (C) For the combination of both odors, healthy controls showed higher activation in parts of insula bilaterally and for parts of the right orbitofrontal cortex. The right orbitofrontal cortex is annotated with green. Insula is annotated with blue. Color bars are given in terms of T-statistic and maps are thresholded at $p < .001$ (uncorrected). R: right hemisphere. The spatial brain maps were created with FSLeyes (FMRIB Analysis Group, University of Oxford, UK).

study on whether the olfactory impairment in PD correlates to decreased recruitment of the default, the salience and the central executive networks. ICA of the resting-state data from this cohort identified three networks that corresponded with the salience network, the executive network and the dorsal default mode network. Dual regression analysis, with the UPSIT score serving as covariate, did not reveal any significant differences between PD patients and healthy controls in recruiting these two networks. There was, however, a tendency for positive correlation between the UPSIT score and the recruitment of the central executive network.

ICA of the resting-state fMRI did not identify an olfactory network. The analysis of functional connectivity between the olfactory cortex (anterior and posterior piriform cortex) and two of its main projections (insula and right orbitofrontal cortex) was tested with a different toolbox, which did not yield any significant differences between the two groups. However, PD patients demonstrated impaired olfaction, which was verified both from the UPSIT and from the results of olfactory fMRI. Therefore, one could assume that the functional connectivity within the olfactory network should also be impaired. However, potential changes in the connectivity within the olfactory network appeared to be subtle, at least in this cohort, and resting-state fMRI could not detect them.

### 4.3. Limitations

As with most studies in this field, our cohort is rather small. However, we analyzed a relatively homogeneous group of patients, with a clinical diagnosis of PD, verified olfactory dysfunction and absence of cognitive impairment. Respiration-triggered event-related fMRI designs are proven to yield a stronger activation of the olfactory cortex compared to fixed-timing odor delivery (Wang et al., 2017). Nevertheless, we chose a less complex experimental design with fixed-timing odor delivery, which was previously validated in healthy participants (Georgiopoulos et al., 2018). The lack of significant differences between the two groups in the activation of olfactory cortex, when analyzed with the GLM, could be partially attributed to the fixed-timing odor delivery; a combination with visual cuing prior to odor presentation could potentially be beneficial in future studies (Moessnang et al., 2011). Another limitation relies in the fact that motion correction of the resting-state fMRI data, as performed with the default pre-processing pipeline of the CONN toolbox, did not include 24 motion parameters, as proposed by Satterthwaite et al. (Satterthwaite et al., 2013). Given the small size of this cohort, we deliberately chose not to include 24 motion parameters as regressors in order to avoid inducing artificial statistical significance.

### 4.4. Conclusions

ICA of olfactory fMRI shows evidence that olfactory impairment in PD is associated with significantly lower recruitment of the olfactory network. GLM analysis revealed significant differences between PD patients and healthy controls in the activation pattern of olfactory projections (insula and right orbitofrontal cortex), but not in the olfactory cortex itself. Hence, ICA was more effective than GLM for studying the differences in the olfactory activation pattern between PD and healthy controls in this cohort, which could be attributed to brain region-dependent, subject-dependent or thresholding variations. Previous studies in in this field have solely relied on GLM analysis, leading to inconsistent results. We, therefore, recommend the combination of both ICA and GLM in future studies of olfactory fMRI in PD. Resting-state fMRI did not detect any significant changes in the functional connectivity within the olfactory network of PD patients without cognitive impairment. Future studies in the different subtypes of PD (e.g. PD with mild cognitive impairment and PD with de novo depression) can potentially elucidate olfactory related differences in the resting-state networks.

## Declaration of Competing Interest

None.

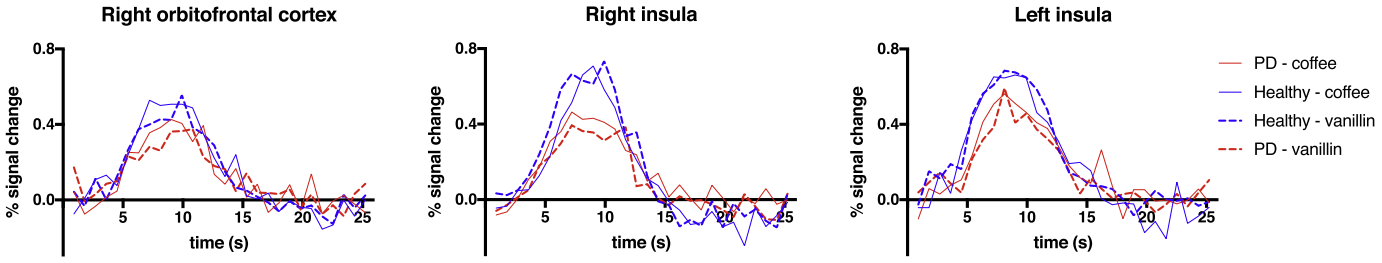


**Fig. 5.** Finite Impulse Response (FIR) event related time courses for insula bilaterally and right orbitofrontal cortex. Healthy controls demonstrated higher maximal signal change and broader area under the curve compared to PD patients. The time courses represent percent signal change of the beta weight. Healthy controls are plotted in blue, PD patients are plotted in red. Coffee is plotted with a continuous line. Vanillin is plotted with a dashed line.

## Acknowledgments

The authors would like to thank Ursula Schmiauke and Jan Schmiauke, from the department of Neurology, Linköping University Hospital, for contributing in the clinical examination of the patients, as well as Charlotte Lundström, research coordinator at the department of Radiology, Linköping University Hospital, for administrative help. This study was supported by the Swedish Parkinson Foundation, Linköping University Hospital Research Fund and by ALF Grants from Region Östergötland.

## References

Abele, M., Riet, A., Hummel, T., Klockgether, T., Wullner, U., 2003. Olfactory dysfunction in cerebellar ataxia and multiple system atrophy. J. Neurol. 250, 1453–1455.
Abou-Elseoud, A., Starck, T., Remes, J., Nikkinen, J., Tervonen, O., Kiviniemi, V., 2010. The effect of model order selection in group PICA. Hum. Brain Mapp. 31, 1207–1216.
Barresi, M., Ciurleo, R., Giacoppo, S., Foti Cuzzola, V., Celi, D., Bramanti, P., Marino, S., 2012. Evaluation of olfactory dysfunction in neurodegenerative diseases. J. Neurol. Sci. 323, 16–24.
Bartels, A., Zeki, S., 2004. The chronoarchitecture of the human brain–natural viewing conditions reveal a time-based anatomy of the brain. Neuroimage 22, 419–433.
Beckmann, C.F., Smith, S.M., 2004. Probabilistic independent component analysis for functional magnetic resonance imaging. IEEE Trans. Med. Imaging 23, 137–152.
Beckmann, C.F., Smith, S.M., 2005. Tensorial extensions of independent component analysis for multisubject FMRI analysis. Neuroimage 25, 294–311.
Bohnen, N.I., Gedela, S., Kuwabara, H., Constantine, G.M., Mathis, C.A., Studenski, S.A., Moore, R.Y., 2007. Selective hyposmia and nigrostriatal dopaminergic denervation in Parkinson's disease. J. Neurol. 254, 84–90.
Bohnen, N.I., Gedela, S., Herath, P., Constantine, G.M., Moore, R.Y., 2008. Selective hyposmia in Parkinson disease: association with hippocampal dopamine activity. Neurosci. Lett. 447, 12–16.
Brand, G., 2006. Olfactory/trigeminal interactions in nasal chemoreception. Neurosci. Biobehav. Rev. 30, 908–917.
Buckner, R.L., Andrews-Hanna, J.R., Schacter, D.L., 2008. The brain's default network: anatomy, function, and relevance to disease. Ann. N. Y. Acad. Sci. 1124, 1–38.
Chang, Y.T., Lu, C.H., Wu, M.K., Hsu, S.W., Huang, C.W., Chang, W.N., Lien, C.Y., Lee, J.J., Chang, C.C., 2017. Salience network and depressive severities in Parkinson's disease with mild cognitive impairment: a structural covariance network analysis. Front. Aging Neurosci. 9, 417.
Connelly, T., Farmer, J.M., Lynch, D.R., Doty, R.L., 2003. Olfactory dysfunction in degenerative ataxias. J. Neurol. Neurosurg. Psychiatry 74, 1435–1437.
Davidsson, A., Georgiopoulos, C., Dizdar, N., Granerus, G., Zachrisson, H., 2014. Comparison between visual assessment of dopaminergic degeneration pattern and semi-quantitative ratio calculations in patients with Parkinson's disease and atypical Parkinsonian syndromes using DaTSCAN(R) SPECT. Ann. Nucl. Med. 28, 851–859.
Disbrow, E.A., Carmichael, O., He, J., Lanni, K.E., Dressler, E.M., Zhang, L., Malhado-Chang, N., Sigvardt, K.A., 2014. Resting state functional connectivity is associated with cognitive dysfunction in non-demented people with Parkinson's disease. J. Park. Dis. 4, 453–465.
Doty, R.L., Brugger, W.E., Jurs, P.C., Orndorff, M.A., Snyder, P.J., Lowry, L.D., 1978. Intranasal trigeminal stimulation from odorous volatiles: psychometric responses from anosmic and normal humans. Physiol. Behav. 20, 175–185.
Doty, R.L., Deems, D.A., Stellar, S., 1988. Olfactory dysfunction in parkinsonism: a general deficit unrelated to neurologic signs, disease stage, or disease duration. Neurology 38, 1237–1244.
Georgiopoulos, C., Witt, S.T., Haller, S., Dizdar, N., Zachrisson, H., Engstrom, M., Larsson, E.M., 2018. Olfactory fMRI: implications of stimulation length and repetition time. Chem. Senses 43, 389–398.
Gottfried, J.A., 2010. Central mechanisms of odour object perception. Nat. Rev. Neurosci. 11, 628–641.
Hahner, A., Maboshe, W., Baptista, R.B., Storch, A., Reichmann, H., Hummel, T., 2013. Selective hyposmia in Parkinson's disease? J. Neurol. 260, 3158–3160.
Harding, A.J., Stimson, E., Henderson, J.M., Halliday, G.M., 2002. Clinical correlates of selective pathology in the amygdala of patients with Parkinson's disease. Brain 125, 2431–2445.
van Hartevelt, T.J., Kringelbach, M.L., 2012. The olfactory system. In: Mai, J.K., Paxinos, G. (Eds.), The Human Nervous System. Elsevier Academic Press, Amsterdam; Boston, pp. 1219–1238.
Hawkes, C.H., Shephard, B.C., Daniel, S.E., 1997. Olfactory dysfunction in Parkinson's disease. J. Neurol. Neurosurg. Psychiatry 62, 436–446.
Hawkes, C.H., Shephard, B.C., Daniel, S.E., 1999. Is Parkinson's disease a primary olfactory disorder? QJM 92, 473–480.
Hou, Y., Yang, J., Luo, C., Song, W., Ou, R., Liu, W., Gong, Q., Shang, H., 2016. Dysfunction of the default mode network in drug-naive Parkinson's disease with mild cognitive impairments: a resting-state fMRI study. Front. Aging Neurosci. 8, 247.
Hummel, T., Fliessbach, K., Abele, M., Okulla, T., Reden, J., Reichmann, H., Wullner, U., Haehner, A., 2010a. Olfactory FMRI in patients with Parkinson's disease. Front. Integr. Neurosci. 4, 125.
Hummel, T., Witt, M., Reichmann, H., Welge-Luessen, A., Haehner, A., 2010b. Immunohistochemical, volumetric, and functional neuroimaging studies in patients with idiopathic Parkinson's disease. J. Neurol. Sci. 289, 119–122.
Hyvarinen, A., 1999. Fast and robust fixed-point algorithms for independent component analysis. IEEE Trans. Neural Netw. 10, 626–634.
Kadohisa, M., Wilson, D.A., 2006. Separate encoding of identity and similarity of complex familiar odors in piriform cortex. Proc. Natl. Acad. Sci. U. S. A. 103, 15206–15211.
Kahraman, D., Eggers, C., Schicha, H., Timmermann, L., Schmidt, M., 2012. Visual assessment of dopaminergic degeneration pattern in 123I-FP-CIT SPECT differentiates patients with atypical parkinsonian syndromes and idiopathic Parkinson's disease. J. Neurol. 259, 251–260.
Karunanayaka, P.R., Lee, E.Y., Lewis, M.M., Sen, S., Eslinger, P.J., Yang, Q.X., Huang, X., 2016. Default mode network differences between rigidity- and tremor-predominant Parkinson's disease. Cortex 81, 239–250.
Karunanayaka, P.R., Wilson, D.A., Tobia, M.J., Martinez, B.E., Meadowcroft, M.D., Eslinger, P.J., Yang, Q.X., 2017. Default mode network deactivation during odor-visual association. Hum. Brain Mapp. 38, 1125–1139.
Kohli, P., Soler, Z.M., Nguyen, S.A., Muus, J.S., Schlosser, R.J., 2016. The association between olfaction and depression: a systematic review. Chem. Senses 41, 479–486.
Lucas-Jimenez, O., Ojeda, N., Pena, J., Diez-Cirarda, M., Cabrera-Zubizarreta, A., Gomez-Esteban, J.C., Gomez-Beldarrain, M.A., Ibarretxe-Bilbao, N., 2016. Altered functional connectivity in the default mode network is associated with cognitive impairment and brain anatomical changes in Parkinson's disease. Parkinsonism Relat. Disord. 33, 58–64.
Mainland, J., Sobel, N., 2006. The sniff is part of the olfactory percept. Chem. Senses 31, 181–196.
Menon, V., 2011. Large-scale brain networks and psychopathology: a unifying triple network model. Trends Cogn. Sci. 15, 483–506.
Moessnang, C., Frank, G., Bogdahn, U., Winkler, J., Greenlee, M.W., Klucken, J., 2011. Altered activation patterns within the olfactory network in Parkinson's disease. Cereb. Cortex 21, 1246–1253.
Morrot, G., Bonny, J.M., Lehallier, B., Zanca, M., 2013. fMRI of human olfaction at the individual level: interindividual variability. J. Magn. Reson. Imaging 37, 92–100.
Nickerson, L.D., Smith, S.M., Ongur, D., Beckmann, C.F., 2017. Using dual regression to investigate network shape and amplitude in functional connectivity analyses. Front. Neurosci. 11, 115.
Paschen, L., Schmidt, N., Wolff, S., Cnyrim, C., van Eimeren, T., Zeuner, K.E., Deuschl, G., Witt, K., 2015. The olfactory bulb volume in patients with idiopathic Parkinson's disease. Eur. J. Neurol. 22, 1068–1073.
Pasquier, F., Leys, D., Weerts, J.G., Mounier-Vehier, F., Barkhof, F., Scheltens, P., 1996. Inter- and intraobserver reproducibility of cerebral atrophy assessment on MRI scans with hemispheric infarcts. Eur. Neurol. 36, 268–272.
Pellegrino, R., Hahner, A., Bojanowski, V., Hummel, C., Gerber, J., Hummel, T., 2016. Olfactory function in patients with hyposmia compared to healthy subjects - an fMRI study. Rhinology 54, 374–381.
Power, J.D., Barnes, K.A., Snyder, A.Z., Schlaggar, B.L., Petersen, S.E., 2012. Spurious but systematic correlations in functional connectivity MRI networks arise from subject motion. Neuroimage 59, 2142–2154.
Putcha, D., Ross, R.S., Cronin-Golomb, A., Janes, A.C., Stern, C.E., 2015. Altered intrinsic functional coupling between core neurocognitive networks in Parkinson's disease. Neuroimage Clin. 7, 449–455.
Putcha, D., Ross, R.S., Cronin-Golomb, A., Janes, A.C., Stern, C.E., 2016. Salience and default mode network coupling predicts cognition in aging and Parkinson's disease. J. Int. Neuropsychol. Soc. 22, 205–215.
Raichle, M.E., Snyder, A.Z., 2007. A default mode of brain function: a brief history of an evolving idea. Neuroimage 37, 1083–1090 (discussion 1097-1089).
Ray, K.L., McKay, D.R., Fox, P.M., Riedel, M.C., Uecker, A.M., Beckmann, C.F., Smith, S.M., Fox, P.T., Laird, A.R., 2013. ICA model order selection of task co-activation networks. Front. Neurosci. 7, 237.
Reichert, J.L., Postma, E.M., Smeets, P.A.M., Boek, W.M., de Graaf, K., Schopf, V., Boesveldt, S., 2018. Severity of olfactory deficits is reflected in functional brain networks-an fMRI study. Hum. Brain Mapp. 39, 3166–3177.
Satterthwaite, T.D., Elliott, M.A., Gerraty, R.T., Ruparel, K., Loughead, J., Calkins, M.E., Eickhoff, S.B., Hakonarson, H., Gur, R.C., Gur, R.E., Wolf, D.H., 2013. An improved framework for confound regression and filtering for control of motion artifact in the preprocessing of resting-state functional connectivity data. Neuroimage 64, 240–256.
Seeley, W.W., Menon, V., Schatzberg, A.F., Keller, J., Glover, G.H., Kenna, H., Reiss, A.L., Greicius, M.D., 2007. Dissociable intrinsic connectivity networks for salience processing and executive control. J. Neurosci. 27, 2349–2356.
Seubert, J., Freiherr, J., Djordjevic, J., Lundstrom, J.N., 2013. Statistical localization of human olfactory cortex. Neuroimage 66, 333–342.
Siderowf, A., Jennings, D., Connolly, J., Doty, R.L., Marek, K., Stern, M.B., 2007. Risk factors for Parkinson's disease and impaired olfaction in relatives of patients with Parkinson's disease. Mov. Disord. 22, 2249–2255.
Silveira-Moriyama, L., Holton, J.L., Kingsbury, A., Ayling, H., Petrie, A., Sterlacci, W., Poewe, W., Maier, H., Lees, A.J., Revesz, T., 2009. Regional differences in the severity of Lewy body pathology across the olfactory cortex. Neurosci. Lett. 453, 77–80.
Smeets, M.A., Veldhuizen, M.G., Galle, S., Gouweloos, J., de Haan, A.M., Vernooij, J., Visscher, F., Kroeze, J.H., 2009. Sense of smell disorder and health-related quality of life. Rehabil. Psychol. 54, 404–412.
Smith, S.M., Fox, P.T., Miller, K.L., Glahn, D.C., Fox, P.M., Mackay, C.E., Filippini, N., Watkins, K.E., Toro, R., Laird, A.R., Beckmann, C.F., 2009. Correspondence of the brain's functional architecture during activation and rest. Proc. Natl. Acad. Sci. U. S. A. 106, 13040–13045.
Sobel, N., Prabhakaran, V., Hartley, C.A., Desmond, J.E., Zhao, Z., Glover, G.H., Gabrieli, J.D., Sullivan, E.V., 1998. Odorant-induced and sniff-induced activation in the cerebellum of the human. J. Neurosci. 18, 8990–9001.
Sobel, N., Thomason, M.E., Stappen, I., Tanner, C.M., Tetrud, J.W., Bower, J.M., Sullivan, E.V., Gabrieli, J.D., 2001. An impairment in sniffing contributes to the olfactory

impairment in Parkinson's disease. Proc. Natl. Acad. Sci. U. S. A. 98, 4154–4159.
Su, M., Wang, S., Fang, W., Zhu, Y., Li, R., Sheng, K., Zou, D., Han, Y., Wang, X., Cheng, O., 2015. Alterations in the limbic/paralimbic cortices of Parkinson's disease patients with hyposmia under resting-state functional MRI by regional homogeneity and functional connectivity analysis. Parkinsonism Relat. Disord. 21, 698–703.
Tissingh, G., Berendse, H.W., Bergmans, P., DeWaard, R., Drukarch, B., Stoof, J.C., Wolters, E.C., 2001. Loss of olfaction in de novo and treated Parkinson's disease: possible implications for early diagnosis. Movement Disord. 16, 41–46.
Vasavada, M.M., Martinez, B., Wang, J., Eslinger, P.J., Gill, D.J., Sun, X., Karunanayaka, P., Yang, Q.X., 2017. Central olfactory dysfunction in Alzheimer's disease and mild cognitive impairment: a functional MRI study. J. Alzheimers Dis. 59, 359–368.
Wahlund, L.O., Barkhof, F., Fazekas, F., Bronge, L., Augustin, M., Sjogren, M., Wallin, A., Ader, H., Leys, D., Pantoni, L., Pasquier, F., Erkinjuntti, T., Scheltens, P., European Task Force on Age-Related White Matter, C, 2001. A new rating scale for age-related white matter changes applicable to MRI and CT. Stroke 32, 1318–1322.
Wang, J., Eslinger, P.J., Smith, M.B., Yang, Q.X., 2005. Functional magnetic resonance imaging study of human olfaction and normal aging. J. Gerontol. A Biol. Sci. Med. Sci. 60, 510–514.
Wang, J., Rupprecht, S., Sun, X., Freiberg, D., Crowell, C., Cartisano, E., Vasavada, M., Yang, Q.X., 2017. A free-breathing fMRI method to study human olfactory function. J. Vis. Exp. 125, e54898. https://doi.org/10.3791/54898.
Welge-Lussen, A., Wattendorf, E., Schwerdtfeger, U., Fuhr, P., Bilecen, D., Hummel, T., Westermann, B., 2009. Olfactory-induced brain activity in Parkinson's disease relates to the expression of event-related potentials: a functional magnetic resonance imaging study. Neuroscience 162, 537–543.
Westermann, B., Wattendorf, E., Schwerdtfeger, U., Husner, A., Fuhr, P., Gratzl, O., Hummel, T., Bilecen, D., Welge-Lussen, A., 2008. Functional imaging of the cerebral olfactory system in patients with Parkinson's disease. J. Neurol. Neurosurg. Psychiatry 79, 19–24.
Whitfield-Gabrieli, S., Nieto-Castanon, A., 2012. Conn: a functional connectivity toolbox for correlated and anticorrelated brain networks. Brain Connect 2, 125–141.
Zatorre, R.J., Jones-Gotman, M., Rouby, C., 2000. Neural mechanisms involved in odor pleasantness and intensity judgments. Neuroreport 11, 2711–2716.